5-2017

Performance Testing and Analysis of Synchronous Reluctance Motor Utilizing Dual-phase Magnetic Material

Patel B. Reddy
General Electric

Ayman M. EL-Refaie
Marquette University, ayman.el-refaie@marquette.edu

Min Zou
General Electric

Di Pan
General Electric

James P. Alexander
General Electric

See next page for additional authors

Performance Testing and Analysis of Synchronous Reluctance Motor Utilizing Dual-phase Magnetic Material

Patel B. Reddy
General Electric; Global Research Center. Niskayuna, NY
Ayman El-Refaie
Marquette University; Electrical & Computer Engineering Dept., Milwaukee, WI
Min Zou
General Electric; Global Research Center. Niskayuna, NY
Di Pan
General Electric; Global Research Center. Niskayuna, NY
James P. Alexander
General Electric; Global Research Center. Niskayuna, NY
Nidhishri Tapadia
General Electric; Global Research Center. Niskayuna, NY
Kevin Grace
General Electric; Global Research Center. Niskayuna, NY

Kum-kang Huh
General Electric; Global Research Center. Niskayuna, NY
Frank Johnson
General Electric; Global Research Center. Niskayuna, NY

Abstract:

While interior permanent magnet (1PM) machines have been considered the state-of-the art for traction motors, synchronous reluctance (SynRel) motors with advanced materials can provide a competitive alternative. 1PM machines typically utilize Neodymium 1ron Boron (NdFeB) permanent magnets, which pose an issue in terms of price, sustainability, demagnetization at higher operating temperatures, and uncontrolled generation. On the other hand, SynRel machines do not contain any magnets and are free from these issues. However, the absence of magnets as well the presence of bridges and centerposts limit the flux-weakening capability of a SynRel machine and limit the achievable constant power speed ratio (CPSR) without having to significantly oversize the machine and/or the power converter. 1n this paper, a new material referred to as the dual-phase magnetic material where nonmagnetic regions can be selectively introduced within each lamination will be evaluated for SynRel designs. The dual-phase feature of this material enables non-magnetic bridges and posts, eliminating one of the key limitations of the SynRel designs in terms of torque density and flux-weakening. This paper will present, the design, analysis and test results of an advanced proof-of-concept SynRel design utilizing dual-phase material with traction applications as the ultimate target application.

SECTION I. Introduction

While interior permanent magnet (IPM) machines have been the primary candidates for traction motors in light-duty HEV/EV, the price and availability of rare-earth materials used in permanent magnets have been a cause of concern. Typically these motors usually use Neodymium Iron Boron (NdFeB) permanent magnets, which contain both light rare earth materials such as Neodymium (Nd) as well as heavy rare-earth materials such as Dysprosium (Dy). One of the key risks in terms of using these rare-earth magnets is the significant fluctuation/increase in their prices as well as their sustainability over the past few years. Industries that use large quantities of these magnets especially traction and wind generator applications were the most affected by these fluctuations. There has been an ongoing global effort to try to reduce or eliminate the use of rare earth materials without sacrificing performance too much. As a part of reduction/elimination of rare-earth materials, conventional topologies such as induction, switched reluctance, and synchronous reluctance (SynRel) are being considered as alternatives.

SynRel machines are particularly appealing due to their smooth and simple passive rotor structure, comparable power density to induction motors [5], [8], [10], [12]–[13][14], low rotor losses and synchronous operation/simple control [6], [7], [11]. The key disadvantages of the SynRel machine are low power factor and typically limited constant power speed ratio (CPSR) [9]. This is mainly due to the presence of bridges and/or center-posts, especially in high-speed machines.

In this paper, design, analysis and test results of a novel proof-of-concept synchronous reluctance design utilizing a dual phase material that has been internally developed within GE will be presented. The key novelty in that design is that it eliminates the need for electromagnetic bridges as well as being suitable for high-speed operation (the dual-phase material is only used for rotor laminations). These results are compared against a SynRel rotor built with conventional silicon steel (HF10) laminations.

SECTION II. Dual-Phase Material

The concept of dual-phase magnetic material is to have a magnetic material that by local treatment can introduce nonmagnetic regions. GE internally developed such a material. The details of the material composition and the process to achieve the local non-magnetic regions are included in [15]. The two phases of the material in an example of a SynRel design are shown in Figure 1. The green regions in the design represent the magnetic phase of the material, while the red regions represent the non-magnetic phase of the material. By choosing to make the bridges and the center-posts nonmagnetic regions, this will have a significant impact on addressing the challenges of SynRel machines previously highlighted.

The non-magnetic bridges and centerposts can withstand mechanical stresses due to high tip-speeds without minimum penalty in terms of magnets leakage flux in those regions. The magnetic regions have yield strength of 40 ksi while the nonmagnetic regions have yield strength of 82 ksi, which further helps reduce the thickness of the bridges and posts. Fig. 2 shows a proof-of-concept lamination and as explained in the figure, by using magnetic paper, it can be seen that the bridges and posts show up as non-magnetic similar to the air cavities.

One of the challenges of the dual-phase material is the low magnetic saturation limit of 1.5 T, which comes as a byproduct of using the new magnetic alloy. While the leakage of magnetic flux into the bridges and center-posts is reduced/eliminated, the lower saturation limit places a constraint on the maximum rotor flux and hence the power capability of the machine. Depending on the design specifications and especially in the case of high-speed machines, the benefits of having non-magnetic bridges and centerposts more than offset the impact of the lower saturation level.

Figure 1: Cross-section of synchronous reluctance design using dual phase material, red-non-magnetic, green-magnetic

SECTION III. Synchronous Reluctance (SynRel) Motor with Dual-Phase Materials

A standard off-the-shelf 5 HP, 6-pole GE Induction motor “5KS215SAA308C” is utilized for the prototyping effort using the dual phase material. The rotor of the induction motor is replaced with two different SynRel rotors to understand the effect of the change in laminations - a Dual-Phase (DP) laminated rotor with non-magnetic bridges and centerposts (Figure 3) and a conventional (using silicon steel HF10) laminated rotor with magnetic bridges and centerposts (Figure 4). Both rotors are designed to handle centrifugal stresses up to mechanical speed of 14000 rpm, which represents the maximum speed in the final prototype. The HF10 rotor requires quite

thick bridges and posts, to be able to withstand mechanical stresses at this speed. On the other hand, in the DP rotor, while the same speed applies, the key advantages lie in the ability to turn these bridges and posts into non-magnetic regions. The use of non-magnetic regions in the rotor helps reduce the leakage inductance in the motor, thereby improving the saliency and hence the torque performance as well as flux weakening or high speed performance of the motor. The laminations made out of the dual-phase material are shown in Fig. 5 while the fully-assembled motor is shown in Fig. 6.

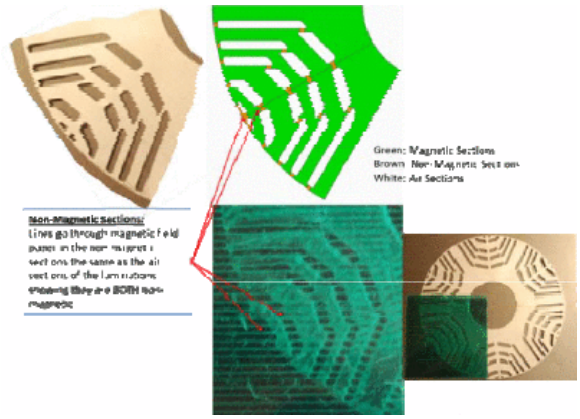

Figure 2: Proof-of-concept lamination showing the magnetic and non-magnetic regions

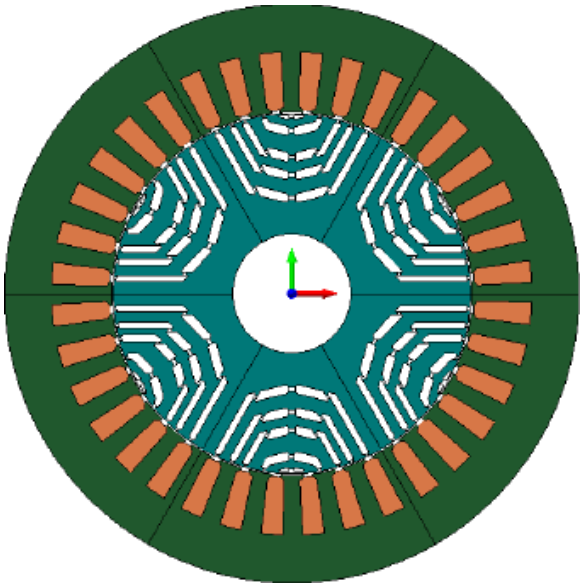
Figure 3: Synchronous reluctance (SynRel) motor with dual-phase laminations

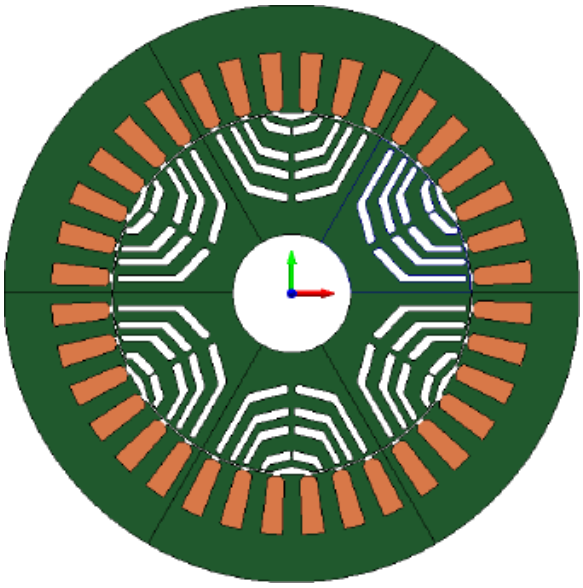

Figure 4: SynRel motor with conventional (HF10) laminations

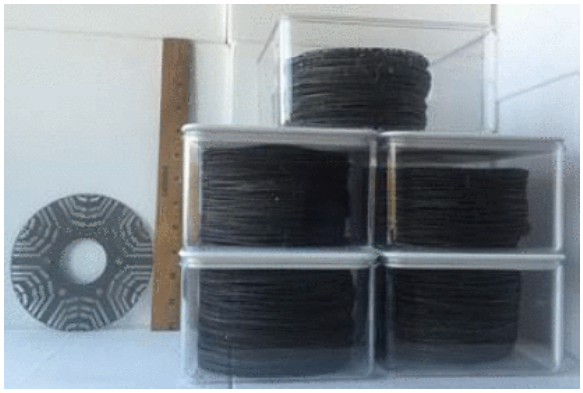

Figure 5: The final stack of dual-phase laminations

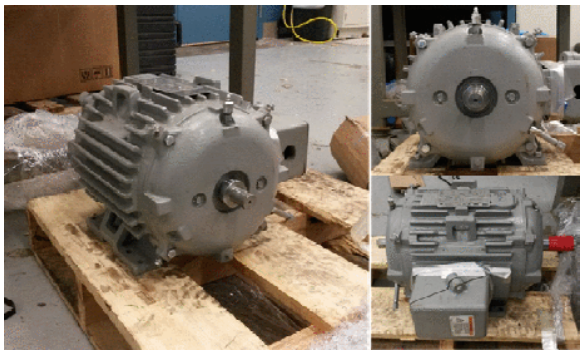

Figure 6: Fully assembled test motor with dual-phase laminations

SECTION IV. Initial Analysis Results

With the new rotors, the torque vs. current and the torque vs. speed predictions are shown in Fig. 7 and Fig. 8 respectively. The use of dual-phase materials on the rotor is expected to improve the torque (and shear stress) by a maximum of 20% (equivalent of 1.5 psi improvement), at about 60 Arms, equivalent to an electric loading of 188 kA/m. This is a significant improvement in torque, since the electric loading of 188 kA/m, is close to the peak electric loading of 200 kA/m in most of state-of-art traction motors. This goes to say that use of dual-phase materials should improve the power density of the motor as well. Such power density improvement might not be expected because the dual phase materials have a lower saturation flux density compared the HF10

laminations, but the use of the dual-phase laminations only on the rotor works around that problem. In other words, since the saturation levels of flux densities on the rotor are lower, the lower saturation property of the dual-phase material is not an issue.

The power density improvement comes mainly from the saliency improvement. Use of the dual-phase material allows for the bridges and posts to function as non-magnetic for the electromagnetic performance. Because torque in the synchronous reluctance motors is directly proportional to saliency, an improvement in saliency is beneficial to the torque production.

On the other hand, the flux weakening performance is a voltage constrained case and benefits from the reduction of the flux leakage. This is enabled by the non-magnetic bridges and posts in the dual-phase motor. As a consequence, the DP rotor is expected to outperform the HF10 rotor, as seen in Fig. 8.

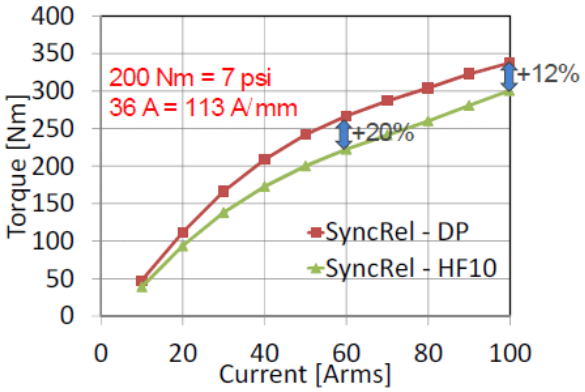

Figure 7: Torque vs. Current curves of DP and HF10 motors

SECTION V. Mechanical Analysis

A finite element model was constructed to calculate the angular velocity at which failure would be expected to occur. The model used the material properties that were measured during the alloy development process. Figure 9 shows the finite element model that was used to calculate the deflection experienced by the laminate during spin testing. All calculations used room temperature properties as the spin test was only conducted at room temperature as will be discussed in the following section. Figure 10 plots the calculated plastic strain as a function of rotational speed. Failure of the laminate is predicted to occur at a speed of 24,500 rpm.

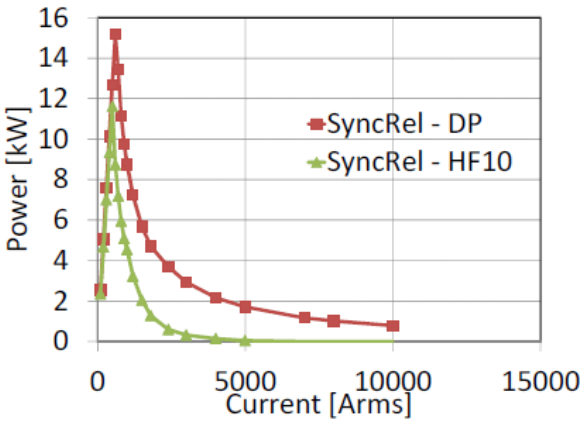

Figure 8: Power vs. Speed curves of DP and HF10 motors

Figure 11 plots the calculated distribution of stress in the laminates both in the as-manufactured state as well as when being rotated at a rotational speed of 19,400 rpm. Residual compressive stress is predicted to be present

in the laminates after manufacturing due to differential thermal expansion between the magnetic and non-magnetic regions after cooling down from the nitriding temperature which is part of the process to introduce the non-magnetic regions.

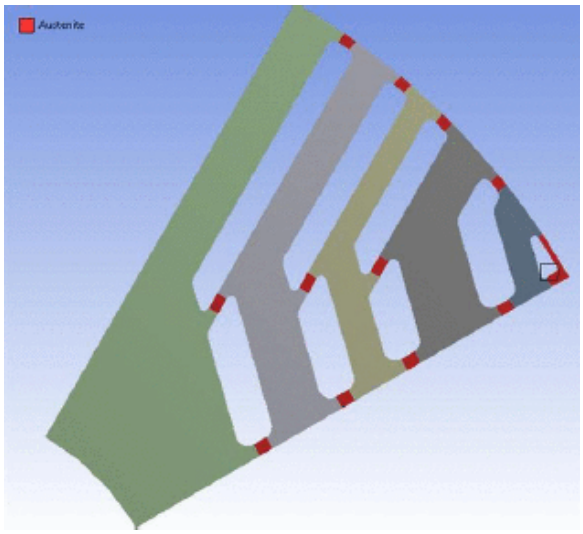

Figure 9: The finite element model used to calculate deflection and yield points during spin testing.

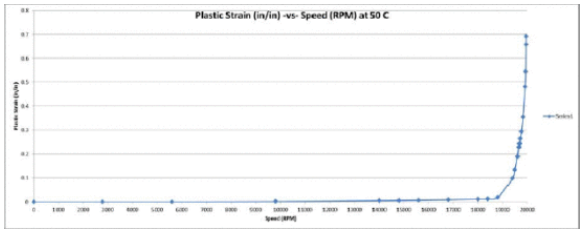

Figure 10: Plastic strain as a function of rotational speed. This calculation predicts that failure will occur at a speed of 24,500 rpm.

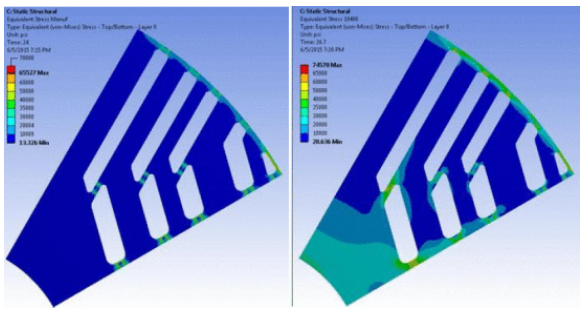

Figure 11: Stress distribution in laminates in the as-manufactured state (left) and while being rotated at a speed 19,400 of rpm.

SECTION VI. Rotor Spin Test

The next step was a spin test to verify the ability of the dual-phase lamination to survive the mechanical stresses encountered during operation of the motor. Previous tensile tests of dual-phase coupons verified the ability of the interface between the magnetic and non-magnetic regions to withstand tensile stress up to the yield stress of the (stronger) nonmagnetic region. However, it was unknown if a fully patterned lamination would have a similar ability to withstand tensile stress. This risk was deemed high enough to warrant the assembly of a subscale stack of laminates that could be subjected to a spin test to failure under controlled conditions. Figure 12 shows two views of the laminations stack on the test stand. The laminations were mounted onto a shaft and held in place with end plates. Eddy current probes were mounted at the perimeter of the laminate to measure

deflection during the test. The test was conducted at room temperature in vacuum. Deflection was measured at speed increments of 1,000 rpm by going to progressively higher test speeds and then returning to a speed of 2,500 rpm between test points. Deflections of the outer diameter were measured at each speed point and then at 2,500 rpm between test points. This was done to measure the onset of plastic deformation of the laminates. The actual deflection for each speed increment is the difference between the high speed (elastic+plastic) and low speed (mostly plastic) deflections. A high speed camera was used to record the laminates at the moment of failure.

Figure 13 compares the measured and calculated deflection of the laminates. Failure of the laminates is observed to occur at a speed of 26,200 rpm. This compares favorably to the calculated failure speed of 24,500 rpm. Figure 14 is a still image from the high speed video taken at the moment of failure of the lamination stack at 26,200 rpm. One pole of one of the laminations is observed to be liberated and is exiting the stack in the lower right of the image.

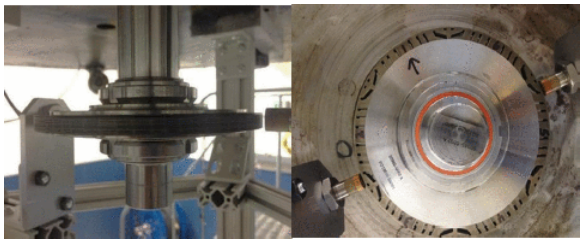

Figure 12: Two views of the laminate stack as mounted on the test stand. Two eddy current probes are located at the outer perimeter of the laminate stack.

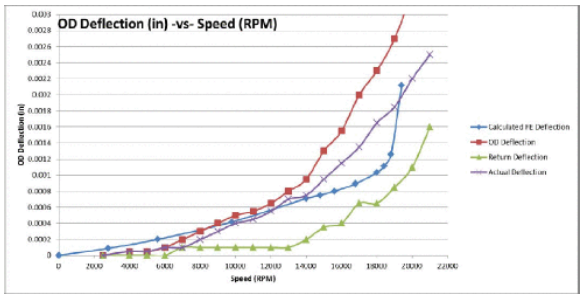

Figure 13: Plot of calculated and measured deflection of the outer diameter as a function of speed.

Figure 14: Still image from high speed camera at the moment of failure of the laminate stack at 26,200 rpm.

Figure 15 and Figure 16 show individual laminations that were removed from the stack after disassembly. The laminations all appear to have failed at bridges and posts that were attached to large cross-section “arms” emanating from the central portion of the laminations.

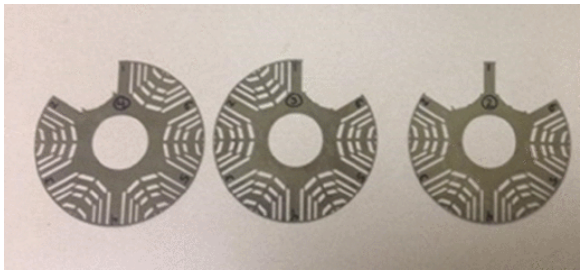

Figure 15: Failed laminationa removed from the test stack.

Figure 16: Close-up images of the failed laminates, indicating the point of failure at the bridges and posts.

SECTION VII. Test Results

Two prototypes having two different rotors (one using dual-phase material and the other using HF10) while having similar stators are tested to determine their torque-speed performance under flux weakening conditions. Since direct torque measurement was unavailable, the torque is estimated from the difference of the input power into the motor and the sum of mechanical, copper and core losses in the motor. Since the operating currents and voltages as well as the stators are similar, it is expected that these loss components are similar in both SynRel rotors.

To impose similar flux weakening conditions, the voltage is kept similar up to a measurable degree between the two rotors and is shown in Figure 17. The torque-speed performance of the conventional (HF10) rotor is overlaid with the dual-phase rotor in Figure 18. Clearly the dual-phase rotor outperforms the conventional rotor from

speeds of 600 rpm to 2000 rpm (flux-weakening region) and beyond and in some cases, the torque capability of the dual-phase rotor is almost 2X compared to that of the HF10 conventional rotor.

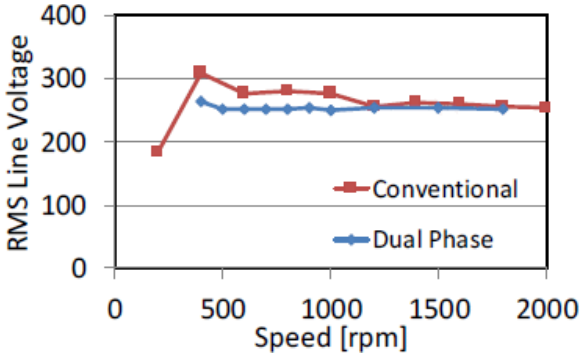

Figure 17: Overlay of the measured rms line voltage of the two motors under flux-weakening

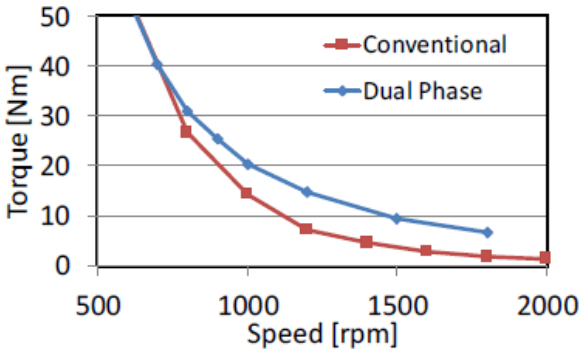

Figure 18: Overlay of the measured torque of the two motors under flux-weakening

In order to have better comparison between the measured and predicted results, The saturation magnetization data is measured in various regions of the excess laminations (after the local nitriding process) and the results are very insightful of the lamination quality. Figure 19 shows the measured magnetization data in the various regions of the laminations.

It is very clear that the dual-phase lamination suffers from the following problems/defects arising from the process control of the nitriding and lamination manufacturing process-(1) Reduced Magnetization in Q-axis path due to Rolling Defects, (2) Reduced Magnetization in channels due to issue of retention of Austenite in the Magnetic Regions as well as nonuniform temperatures (center of the lamination being the hottest and outer edges not receiving enough heat, which shows up in the level of magnetization in the lamination), (3)-Increased Magnetization in bridges and center-posts due to incomplete nitriding process. All of these scale-up processing issues are being addressed and a second round of building and testing a prototype is planned based on improved lamination properties.

Based on the new magnetization data shown in Figure 18, the FEA model is updated with various material properties and is shown in 20. The color of the various regions is based on the level of saturation flux density, with the dark brown being the region with the highest saturation flux density and white being the region with the lowest saturation flux density.

Figure 21 shows a good agreement between measurements and predictions in case of the HF10 rotor (under low speed/constant torque region). In case of the dual-phase rotor and based on the measured material properties in Figure 18 and FEA model in Figure 19, the torque prediction is compared with the test results under low speed conditions. Figure 22 shows that there is fair agreement between the finite element model and the test results. The test result is seen to be within 12% of the 2D finite element predictions of the model simulations.

The following conclusions are summarized from the testing of the dual-phase and conventional rotors:

- The dual-phase rotor outperforms the conventional rotor under flux weakening conditions, in some cases providing 2X more output power
- Due to some imperfections in the process control, the magnetic regions of the dual-phase rotor are impacted. This led to a lower than expected torque-current performance of the dual-phase rotor
- The **main** aspect of the dual-phase laminations that was proved is the ability to produce the nonmagnetic regions. This aspect is reflected in the lower leakage inductances and hence in the power-speed performance under the voltage and current constraints.
- It is expected that once the scale-up process is fine-tuned, the performance of the dual-phase rotor will exceed that of the HF10 rotor low speed in addition to the flux-weakening region that was already shown.
- The off-shelf industrial motor that was used as the starting point of this effort, served the purpose as a proof-of-concept. If machines are designed/optimized from scratch based on the dual-phase material properties, the performance entitlement of the dual-phase rotors will be much more significant.

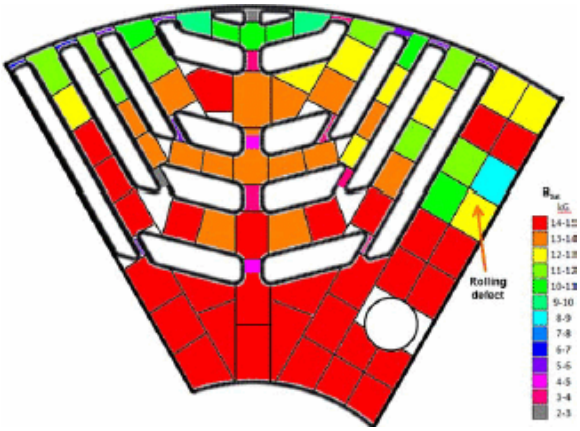

Figure 19: Magnetization data from the material tests in the various magnetic regions of the lamination

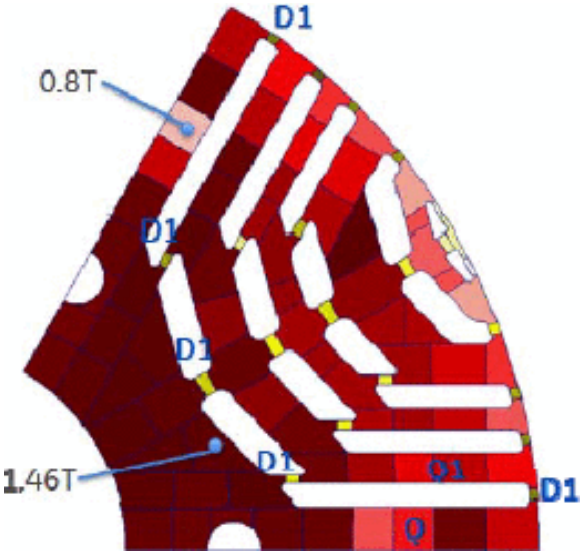

Figure 20: Electromagnetic model of the rotor modeling the various saturation flux densities

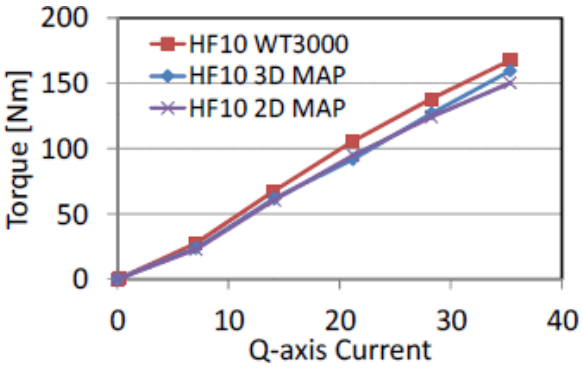

Figure 21: Test vs. predictions with conventional (HF10) laminated rotor

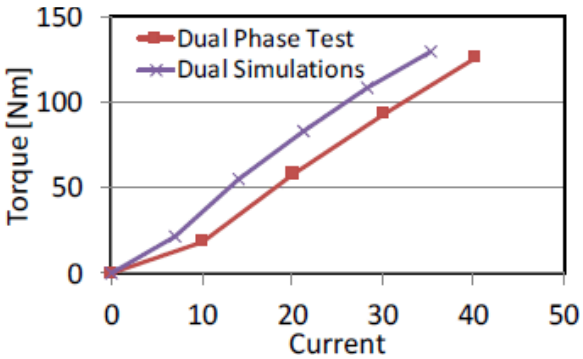

Figure 22: Test results vs. 2D predictions with dual-phase laminated rotor

SECTION VIII. Conclusions

This paper presents the results from the test of a prototype dual-phase laminated rotor, manufactured as a one-to-one replacement of an induction motor rotor. The results show the superiority of the dual-phase rotor over the SynRel rotor made from conventional steel, especially in the flux weakening regions. Some of the aspects arising from the process of the dual-phase manufacturing process are summarized and these are taken into account in the finite element models. The finite element torque predictions compare well with the test results.

The final conclusion is that "**the process of making the dual-phase material is not perfect while the concept of dual-phase has already been proven experimentally**". As previously mentioned, efforts are under way to address all the processing challenges and updated test results based on improved laminations properties will be reported in a future paper.

ACKNOWLEDGMENTS

This material is based upon work supported in part by the Department of Energy, Office of Energy Efficiency and Renewable Energy (EERE), under Award Number DE-EE0007755. This report was prepared as an account of work sponsored by an agency of the United States Government. Neither the United States Government nor any agency thereof, nor any of their employees, makes any warranty, express or implied, or assumes any legal liability or responsibility for the accuracy, completeness, or usefulness of any information, apparatus, product, or process disclosed, or represents that its use would not infringe privately owned rights. Reference herein to any specific commercial product, process, or service by trade name, trademark, manufacturer, or otherwise does not necessarily constitute or imply its endorsement, recommendation, or favoring by the United States Government or any agency thereof. The views and opinions of authors expressed herein do not necessarily state or reflect those of the United States Government or any agency thereof.

References

1. A.M. El-Refaie, J.P. Alexander, S. Galioto, P. Reddy, Kum-Kang Huh, P. de Bock, X. Shen, "Advanced high power-density interior permanent magnet motor for traction applications", *2013 IEEEEnergy Conversion Congress and Exposition (ECCE)*, vol. 50, no. 5, pp. 581-590, 15–19 Sept. 2013.

2. Fang Liang, B.H. Lee, J.J. Lee, H.J. Kim, Jung-Pyo Hong, "Study on high-efficiency characteristics of interior permanent magnet synchronous motor with different magnet material", *Int. Conf. on Electrical Machines and Systems 2009. ICEMS 2009*, pp. 1-4, 15–18 Nov. 2009.

3. P. Sekerak, V. Hrabovcova, J. Pyrhonen, S. Kalamen, P. Rafajdus, M. Onufer, "Comparison of Synchronous Motors With Different Permanent Magnet and Winding Types", *IEEE Trans. on Magnetics*, vol. 49, no. 3, pp. 1256-1263, March 2013.

4. R. Vartanian, Y. Deshpande, H.A. Toliyat, "Performance analysis of a rare earth magnet based NEMA frame Permanent Magnet assisted Synchronous Reluctance Machine with different magnet type and quantity", *IEEE Int. Electric Machines & Drives Conf. (IEMDC) 2013*, pp. 476-483, 12–15 May 2013.

5. T.J.E. Miller, A. Hutton, C. Cossar, D.A. Staton, "Design of a synchronous reluctance motor drive", *IEEE Trans. on Industry Applications*, vol. 27, no. 4, pp. 741-749, Jul/Aug 1991.

6. L Xu, X Xu, T.A. Lipo, D.W. Novotny, "Vector control of a synchronous reluctance motor including saturation and iron loss", *IEEE Trans. on Industry Applications*, vol. 27, no. 5, pp. 977-985, Sep/Oct 1991.

7. R.E. Betz, "Theoretical aspects of control of synchronous reluctance machines", *IEE Proc.s B on Electric Power Applications*, vol. 139, no. 4, pp. 355-364, Jul 1992.

8. A. Vagati, G. Franceschini, I. Marongiu, G.P. Troglia, "Design criteria of high performance synchronous reluctance motors", *Industry Applications Society Annual Meeting 1992*, vol. 1, pp. 66-73, 4–9 Oct 1992.

9. W.L. Soong, T.J.E. Miller, "Theoretical limitations to the field-weakening performance of the five classes of brushless synchronous AC motor drive", *Electrical Machines and Drives 1993. Sixth International Conference on (Conf. Publ. No. 376)*, pp. 127-132, 8–10 Sep 1993.

10. R. Lagerquist, I. Boldea, T.J.E. Miller, "Sensorless-control of the synchronous reluctance motor", *Industry Applications IEEE Transactions on*, vol. 30, no. 3, pp. 673-682, May/Jun 1994.

11. T. Matsuo, T.A. Lipo, "Rotor design optimization of synchronous reluctance machine", *Energy Conversion IEEE Transactions on*, vol. 9, no. 2, pp. 359-365, Jun 1994.

12. A. Vagati, "The synchronous reluctance solution: a new alternative in AC drives", *Industrial Electronics Control and Instrumentation 1994. IECON '94. 20th International Conference on*, vol. 1, no. 1, pp. 1-13, 5–9 Sep 1994.

13. D.A. Staton, W.L. Soong, T.J.E. Miller, "Unified theory of torque production in switched reluctance and synchronous reluctance motors", *Industry Applications IEEE Transactions on*, vol. 31, no. 2, pp. 329-337, Mar/Apr 1995.

14. S.J. Galioto, P.B. Reddy, A.M. EL-Refaie, "Effect of magnet types on performance of high speed spoke interior permanent magnet machines designed for traction applications", *Energy Conversion Congress and Exposition (ECCE) 2014 IEEE*, pp. 4513-4522, 14–18 Sept. 2014.

15. *Dual Phase Material Component And Method of Forming*.